IVYSPRING INTERNATIONAL PUBLISHER

Theranostics

2017; 7(18): 4498-4516. doi: 10.7150/thno.17949

Research Paper

Autophagy Maintains the Function of Bone Marrow Mesenchymal Stem Cells to Prevent Estrogen Deficiency-Induced Osteoporosis

Meng Qi[1, 2*], Liqiang Zhang[1, 2*], Yang Ma[1, 2*], Yi Shuai[1, 2], Liya Li[1, 2], Kefu Luo[1, 3], Wenjia Liu[1, 2✉], Yan Jin[1, 2✉]

1. State Key Laboratory of Military Stomatology & National Clinical Research Center for Oral Diseases & Shaanxi International Joint Research Center for Oral Diseases, Center for Tissue Engineering, School of Stomatology, Fourth Military Medical University, Xi'an, China;
2. Xi'an Institute of Tissue Engineering and Regenerative Medicine, Xi'an, China;
3. State Key Laboratory of Military Stomatology & National Clinical Research Center for Oral Diseases & Shaanxi Clinical Research Center for Oral Diseases, Department of Prosthodontics, School of Stomatology, The Fourth Military Medical University, Xi'an, China.

* These authors contributed equally to the study.

✉ Corresponding authors: Yan Jin, Phone: +86-29-84776471, Fax: +86-29-83218039. E-mail: yanjin@fmmu.edu.cn or yanjinfmmu@139.com. Wenjia Liu, Phone: +86-029-84776471, Fax: +86-29-83218039. E-mail: wenjialiu23@163.com

Received: 2016.10.17; Accepted: 2017.09.11; Published: 2017.10.12

Abstract

Rationale: The impaired function of endogenous bone marrow mesenchymal stem cells (BMMSCs) is a determinant in the development of osteoporosis (OP). Recent researches have proved that autophagy plays an important role in maintenance of skeletal phenotype. However, whether autophagy affects the development of OP through regulating the function of BMMSCs remains elusive.

Methods: Ovariectomy (OVX)-induced OP model and sham model were established in 8-week-old C57 mice. The differentiation and immunoregulation properties of BMMSCs from two models were examined by osteogenic/adipogenic induction *in vitro* and treatment of a dextran sulfate sodium (DSS)-induced mice colitis model *in vivo*. We evaluated autophagy activity in sham and OVX BMMSCs by quantitative real time-polymerase chain reaction (qRT-PCR), western blotting, laser confocal microscopy and transmission electron microscopy (TEM). Finally, to testify the effects of rapamycin, short hairpin RNA (shRNA) -BECN1 (shBECN1) and shRNA-ATG5 (shATG5), we performed Alizarin Red staining and Oil Red O staining to detect lineage differentiations of BMMSCs, and carried out micro-CT, calcein staining and Oil Red O staining to assess the skeletal phenotype.

Results: BMMSCs from OVX-induced OP model mice exhibited decreased osteogenic differentiation, increased adipogenic differentiation and impaired immunoregulatory capacity. Furthermore, autophagy decreased both in bone marrow and BMMSCs of osteoporotic mice. Importantly, regulation of autophagy directly affects the functions of BMMSCs, including differentiation and immunoregulatory capacities. Moreover, treatment with rapamycin rescued the function of endogenous BMMSCs and attenuated the osteoporotic phenotype in OVX mice.

Conclusion: Our findings suggest that autophagy regulates the regenerative function of BMMSCs and controls the development of OP. The restoration of autophagy by rapamycin may provide an effective therapeutic method for osteoporosis.

Key words: autophagy, osteoporosis, bone marrow mesenchymal stem cells, regenerative properties.

Introduction

OP is a systemic skeletal disease characterized by microarchitectural deterioration of bone tissue and low bone mass, leading to clinical susceptibility of bone fracture [1, 2]. The prevalence of OP is progressing and affects 34% of women all over the world [3]. Postmenopausal OP, the most common type of OP, is found in one out of three postmenopausal women [4].

BMMSCs are nonhematopoietic multipotent stem cells that play a vital role in maintaining the

bone/marrow homeostasis [5]. Increasing studies have indicated that aberrant lineage differentiation of endogenous BMMSCs contributes to development of OP [6]. Our previous research revealed that elevated TNF-α caused by estrogen withdrawal suppresses miR-21 and consequently disturbs lineage commitment of BMMSCs, leading to OP [7]. Other researchers have also found a similar differentiational favor of adipogenesis overwhelming osteogenesis in BMMSCs from postmenopausal osteoporotic women [8-10]. Additionally, BMMSCs possess not only multipotential differentiation ability, but also prominent immunosuppressive capability, which facilitates clinical application of BMMSCs in immune diseases.

Autophagy is an intracellular degradation system in eukaryotic cells that delivers cytoplasmic components including damaged macromolecules and organelles to the lysosome for degradation and recycling [11, 12]. Autophagy mainly serves as an adaptive process to protect organisms against diverse diseases [13]. During recent years, researchers have pointed out the important role of autophagy in maintenance of bone homeostasis. Deletion of Atg5 in osteoblasts results in decreased bone mass *in vivo*. Knockdown of Atg7 and BECN1 significantly reduces the osteogenic capability of an osteoblastic cell line *in vitro* [14]. Osteoblast-specific deletion of FIP200, which is an essential component of mammalian autophagy, leads to bone loss in mice [15]. Furthermore, a genetic screening study in humans illustrated that, among the various pathways tested, the expression of autophagic-related genes uniquely had a direct relationship with the variation in bone mineral density in the distal portion of the radius in about 1000 individuals [16].

Impaired autophagy has been found in various degenerative diseases, including Alzheimer's disease [17], osteoarthritis [18] and macular degeneration [19]. These findings may highlight the role of autophagy in sustaining function of different cells in various tissues. The relationship between autophagy and pathogenesis of postmenopausal OP, the skeletal degenerative disease, has not been clearly illustrated. Here, we assume that autophagy may modulate regenerative function of endogenous BMMSCs and participate in the development of OP.

Materials and Methods

Ethics statement

All animal procedures were performed and experimental protocols were approved by the guidelines of the Animal Care Committee of the Fourth Military Medical University, Xi'an, China [SCXK(Military) 2007-007], which was in conformity to NIH Guide for the Care and Use of Laboratory Animals.

Animals

All animals were purchased from the Animal Center of Fourth Military Medical University, Xi'an, China. Sixty 8-week-old female C57/BL6 mice were randomly and evenly divided into two groups (thirty in each group) to receive either sham or bilateral ovariectomy (OVX) surgery. Another fifty-five 8-week-old female C57/BL6 mice were used as an experimental colitis model. All mice were housed under specific pathogen-free conditions (22°C, 50%–55% humidity, and 12 h light/12 h dark cycles) with food and water easily accessible.

Establishment of estrogen deficiency-induced OP

Sixty 8-week-old C57/BL6 mice were randomly and evenly divided into sham and OVX groups. After general anesthesia (1% pentobarbital sodium, 30 mg/kg), the mice in the sham group were subjected to resection of some fat tissue close to the ovaries and mice in the OVX group underwent bilateral ovariectomy. Two months later, femurs of mice were isolated after sacrifice for Micro-CT scanning to confirm estrogen deficiency-induced OP was successfully established.

Establishment of experimental colitis model and treatment by injection of BMMSCs

Twenty-five 8-week-old C57/BL6 mice were evenly grouped into five groups at random, including control mice (CON), DSS-induced colitis mice (DSS), DSS-induced colitis mice injected with PBS (DSS+PBS), DSS-induced colitis mice injected with sham BMMSCs (DSS+sham), and DSS-induced colitis mice injected with OVX BMMSCs (DSS+OVX). All mice were fed the same food. The mice in the control group were fed with tri-distilled water. The mice in the other groups were fed with 3% DSS (Millipore, Billerica, MA, USA) for 10 days. On day 3, mice of DSS+sham and DSS+OVX were intravenously administrated with PBS-dissolved cell suspension of sham BMMSCs and OVX BMMSCs, respectively. The mice in the DSS+PBS group were injected with an equal volume of PBS.

Another thirty mice were fed with 3% DSS for 10 days to establish a DSS-induced colitis model. Meanwhile, model mice were evenly distributed into six groups and treated with BMMSCs on day 3, including sham BMMSCs (DSS+sham), sham BMMSCs interfered with scramble RNA (DSS+sham+scr-sh), sham BMMSCs treated with

shBECN1 (DSS+sham+shBECN1), sham BMMSCs with silenced ATG5 via shATG5 (DSS+sham+shATG5), OVX BMMSCs (DSS+OVX), and rapamycin-treated OVX BMMSCs (DSS+OVX+rapamycin). Mortality and body weight were recorded every day. Weight loss, stool formation, and bloody stool were scored daily to determine the disease activity index (DAI). On day 10, the mice were sacrificed. Colon lengths were measured and then fixed for H&E staining.

Isolation and culture of C57B/L BMMSCs

Primary BMMSCs were drawn out by flushing from tibias and femurs of mice with basal culture medium containing α-MEM medium (Gibco, Grand Island, NY, USA), 20% FBS (Sijiqing, Hangzhou, China), 2 mM L-glutamine (Invitrogen, Carlsbad, CA), 100 U/mL penicillin and 100 U/mL streptomycin (Invitrogen, Carlsbad, CA). Single-cell suspension was equally seeded in 9 cm dishes (thermo, Suzhou, China) and initially maintained in an atmosphere of 5% CO_2 at 37°C. The medium was changed on the third day and non-adherent cells were removed with PBS. The adherent cells were cultured with fresh medium for another 6-8 days with medium changed every two days until they were confluent. Then BMMSCs were passaged after digestion with 0.25% trypsin to passage one. BMMSCs at passage one were used for the majority of tests in this research.

Coculture of BMMSCs and T cells

1X10^5 BMMSCs were seeded on a 24-well culture plate and incubated for 24 h. The pre-stimulated T cells were directly loaded onto BMMSCs and co-cultured. 24 h later, T cells were collected for apoptosis analysis.

Evaluation of surface markers by flow cytometry

Five cell surface markers (Sca-1, CD90, CD73, CD34 and CD45) were examined. BMMSCs were trypsinized and counted to ensure each sample had more than 1×10^5 cells. The cells were incubated with antibody anti-Sca-1(FITC) (eBioscience, USA), anti-CD90 (PE) (Biolegend), anti-CD73(FITC) (eBioscience, USA), anti-CD34(PE) (Biolegend, USA) and anti-CD45(PE) (BD Biosciences, USA) for 30 min at room temperature. Then cells were washed twice and suspended for flow cytometry.

Evaluation of apoptosis of BMMSCs

BMMSCs were digested, washed, suspended with PBS and counted to ensure at least 1×10^5 cells in a test. Cell suspension was incubated with Annexin V-FITC and kept away from light for 15 min. Then PI was added to the cells and apoptosis was detected by flow cytometry.

Estrogen treatment *in vitro*

BMMSCs were cultured in α-MEM without phenol red (Life Technologies-Gibco) containing 20% FBS. Hormones in FBS were previously removed by dextran coated charcoal (Sigma, USA). β-estradiol (MP, USA) was added to the media at a range of dosages (0, 0.1, 1, 10, 100, 1000 nM). BMMSCs were collected 48 h later to measure autophagy activity.

Osteogenic and adipogenic induction *in vitro*

To induce BMMSC osteogenic differentiation, BMMSCs were initially cultured in basal growth medium, and switched to osteogenic-inducing medium, containing 60 μg/mL ascorbic acid (Sigma-Aldrich), 2 mM β-glycerophosphate (Sigma-Aldrich) and 10 nM dexamethasone (Sigma-Aldrich), when the cells reached 80% confluence. BMMSCs were seeded into a 6-well plate and a 12-well plate at an initial number of 3×10^5 and 1.5×10^5 per well, respectively. The cells in 6-well plates were cultured in induction medium for 7 days for western blotting assay, and the ones in 12-well plates were induced for 14 days for Alizarin Red staining, respectively. For adipogenic differentiation induction, adipogenic-inducing medium, which contained 0.5 mM isobutylmethylxanthine, 0.5 μM dexamethasone, 10 μg/ml insulin and 60 μM indomethacin (Sigma-Aldrich, St. Louis, MO), was introduced when BMMSCs reached 85%-90% confluence. Cells were induced for 3 days and 7 days, respectively, for western blotting and Oil Red O staining. Both induction media were changed every three days.

Alizarin Red staining

Alizarin Red staining was performed to determine mineralization after 14 days of osteogenic induction. BMMSCs were washed twice with PBS to remove medium and then fixed with 60% isopropanol for 15 min. Then cells were washed gently three times with ddH_2O, followed by staining with 1% Alizarin Red (Sigma Aldrich) for 10 min. Quantitative parameters of the mineralized area were measured with the ImageJ 1.47 software. Percentage of positive area was measured with the ImageJ 1.47 software. The quantification was studied based on semi-automatic plug-ins, which followed the same operational methods.

Oil Red O staining

Oil Red O staining was carried out to detect the lipid droplet formation in adipogenesis [20]. 0.5 g Oil Red O powder (Sigma Chemical Co.) was evenly dissolved in 100 mL of isopropanol to prepare stock

solution, which was then diluted with distilled water at the ratio of 3:2 and filtrated to make working solution [21]. The sections of decalcified femurs and cells were fixed and pre-wetted with 60% isopropanol, and then stained with Oil Red O working solution for 15 min. The positive area was measured with the ImageJ 1.47 software. The quantification was studied based on semi-automatic plug-ins, which followed the same operational methods.

Colony-forming unit (CFU) assays

To assess the capacity and efficiency of cell self-renewal, 5×10^2 primary BMMSCs were evenly seeded in a 5 cm plastic dish with 4 mL α-MEM medium. The medium was refreshed every 3 days. On day 10, cells were rinsed with PBS, fixed by 4% paraformaldehyde, and stained with 0.5% crystal-violet solution for 10 min. Then cells were washed with ddH_20 until the dye stopped coming off, and dried at room temperature. Percentage of positive area was measured with the ImageJ 1.47 software. The quantification was performed based on semi-automatic plug-ins, which followed the same operational methods.

Enzyme-linked Immunosorbent Assay (ELISA)

TNF-α level in serum, and secretory osteoprotegerin (sOPG) and secretory receptor activator of NF-kB ligand (sRANKL) in conditioned medium from BMMSCs were quantified using sandwich ELISA Kits (Yanhui biotechnololy, China), with the sOPG level normalized to sRANKL.

Micro-CT scanning and analysis

Femurs were detached after sacrifice and fixed in 4% paraformaldehyde, then scanned and analyzed by micro-CT (Siemens Inveon, Eschborn, Germany) at a voltage of 80 kV and a current of 500 mA. 1 mm thick area 0.5 mm below the growth plate in the distal ends of the femurs was chosen as the region of interest for trabecular bone analysis.

Double calcein labeling assay

To label new bone formation, mice were subcutaneously injected with calcein (15 mg/kg, Sigma) 10 days and 3 days before sacrifice. After fixation and embedding in polymethyl acrylate, femurs were serially cut into 50 μm thick sections and the double calcein labeling was captured with a fluorescence microscope (Olympus). Osteogenic rate was calculated as inter-label width/labeling period with Image Pro software.

RNA Isolation and transcription-polymerase chain reaction

Total RNA was extracted with TRIzol Reagent (Invitrogen Life Technology, Carlsbad, CA) and 1μg total RNA per sample was reversely transcribed to cDNA using a Prime Script RT reagent kit (TaKaRa, Dalian, China). The primer sequences used are showed in Table 1. The expressions of target genes were quantified by Real-time RT-PCR using the SYBR Premix Ex Taq II kit (TaKaRa) and tested by a CFX96TM Real-time RT-PCR System (Bio-Rad, Hercules, CA, USA). β-actin was used as the housekeeping gene.

Table 1. Primers for Real-time PCR

Gene	Primer sequence
m-LC3-F	CCTGTCCTGGATAAGACCAAGTT
m-LC3-R	CTCCTGTTCATAGATGTCAGCGAT
m-BECN1-F	CAGTACCAGCGGGAGTATAGTGA
m-BECN1-R	TGTGGAAGGTGGCATTGAAGA
m-PPARγ-F	TGTGAGACCAACAGCCTGAC
m-PPARγ-R	AAGTTGGTGGGCCAGAATGG
m-P62-F	CTCTCATAGCCGCTGGCTTC
m-P62-R	CCTCAATGCCTAGAGGGCTG
m-ACTIN-F	CATCCGTAAAGACCTCTATGCCAAC
m-ACTIN-R	ATGGAGCCACCGATCCACA

Protein isolation and western blotting analysis

The samples were lysed in RIPA buffer supplemented with protease inhibitors and subjected to ultrasonics at low frequency. The supernatant containing total proteins was harvested after centrifugation and the protein concentration was measured by bicinchoninic acid protein assay (Beyotime, China). Equal amounts (30 μg) of total proteins were loaded on 10% or 15% SDS-PAGE according to the molecular weight of the target proteins. Proteins were transferred onto polyvinylidene fluoride membranes (Millipore), and blocked in 5% BSA for 2 h at room temperature, followed by incubation overnight at 4°C with primary antibodies for LC3 (Cell Signaling Technology, USA), Beclin1 (Cell Signaling Technology, USA), ATG5 (Cell Signaling Technology, USA), P62 (Proteintech, USA), ALP (R&D systems, USA), Runx2 (Cell Signaling Technology, USA), PPAR-γ (Abcam, UK), OPG (Abcam, UK), RANKL (Abcam, UK) and Actin (Abcam, UK). After rinsed with tris buffered saline supplemented with tween (TBST) three times, membranes were incubated with secondary antibodies (Cowin Biotech Co, Beijing, China) for 1 h at room temperature. Blots were captured with a Western-Light Chemiluminescent Detection System (Tanon, Shanghai, China).

Immunofluorescence analysis

BMMSCs were harvested and coated with 4% paraformaldehyde for 15 min on ice. Femurs were fixed, decalcified and cut into 10 μm thick frozen sections. Cells and bone sections were permeabilized with 0.03% Triton-X100 for 15 mins at room temperature and blocked in 5% BSA at 37°C for 30 min. BMMSCs were incubated with specific primary antibody LC3 (Cell Signaling Technology, USA) and bone sections were stained with LC3 and Sca-1 (Abcam, UK) overnight at 4°C. All samples were then incubated with fluorescent secondary antibodies (Cell Signaling Technology, USA) at room temperature for 2 h after rinsing. Hochest 33342 (Sigma-Aldrich) was used to counterstain cell nuclei at room temperature for 3 min. Stained cells and tissues were observed under a confocal microscope (Olympus).

Transmission Electron Microscopy (TEM) analysis

BMMSCs were digested and washed twice with PBS and primarily fixed in 2.5% glutaraldehyde overnight. Undecalcified bone was cut in to 2 mm cross sections and fixed by the same method. Both were post-fixed in 1% osmium tetroxide for 1h. After washing with PBS, the samples were progressively dehydrated in a graduated series of ethanol solutions (50, 70, 80, 90, 95 and 100%) and embedded in the mixture of Epon 812, DDSA, NMA and DMP-30. Whereafter, bone samples were cut into semi-thin sections (1 μ m), followed by staining with methylene blue for localization in light microscopy. Finally, ultrathin sections (80 nm) were stained with 1% uranyl acetate and lead citrate. The ultrastructure of cells and bone were analyzed with a transmission electron microscope (JEM-1230, Jeol, Japan).

Lentiviral vector construct packaging and transduction

The 3-plasmid expression system was used to generate the lentiviral vectors. The target sequences for shRNA were: BECN1 sh, forward: CCGGCCCTATGGAAATCATTCCTATCTCGAGAT AGGAATGATTTCCATAGGGTTTTTG, reverse: AATTCAAAAACCCTATGGAAATCATTCCTATCT CGAGATAGGAATGATTTCCATAGGG. ATG5 sh, forward: CCGGCCCTGAAATGGCATTATCCAAAT TTCTCGAGAAATTTGGATAATGCCATTTCAGGG TTTTTG, reverse: AATTCAAAAACCCTGAAATGG CATTATCCAAATTTCTCGAGAAATTTGGATAAT GCCATTTCAGGG.The lentivirus was packaged by cotransfecting 293T cells with a transfer vector and two packaging vectors (pMD2.G and psPAX2). 16 h after transfection, the medium was refreshed and cells were cultured for additional 48 h to obtain the supernatant containing virus. The BMMSCs reaching 80% confluence were transduced with lentiviral constructs in the presence of 8 mg/mL polybrene. Cells were harvested 48 h later to detect efficiency of transfection.

Statistical analysis

All the results are displayed as mean ± standard deviation. Comparisons were evaluated by Student's t-test or one-way analysis of variance by Prism software (GraphPad, La Jolla,CA). $P < 0.05$ was considered as significant.

Results

The regenerative capability of BMMSCs is decreased in ovariectomized mice

Initially, we established estrogen deficiency-induced OP by bilateral ovariectomy. The bone mass of femur in OVX mice significantly decreased compared to that of sham mice two months after operation (Fig.S1, A and B). As a previous study has established, interruption of estrogen is associated with the inflammatory process in bone, featured by increasing pro-inflammatory cytokines [22]. The expressions of TNF- α and IL 1-β in serum were compared between sham and OVX mice, and implied an inflammatory skeletal microenvironment in OVX mice (Fig. S1C).

To investigate the underlying cause of bone loss in OVX mice, we isolated sham and OVX BMMSCs and compared the regenerative abilities between them. Firstly, cell phenotypes were detected in BMMSCs via flow cytometric analysis, which revealed the presence of typical BMMSC markers Sca-1, CD73 and CD90, with concomitant absence of CD34 and CD45 in sham and OVX BMMSCs (Fig. S2). As shown in the colony-forming assay, OVX BMMSCs formed fewer CFU than sham BMMSCs (Fig. 1A). Moreover, we confirmed anomalous differentiation commitment of OVX BMMSCs through Alizarin Red staining and Oil Red O staining. As shown in Fig. 1B, OVX BMMSCs formed fewer mineralization nodules, coinciding with the decreased expression of Runx2 and ALP, which are two markers of osteogenesis (Fig. 1C). Meanwhile, more lipid droplets were generated in OVX BMMSCs (Fig. 1D), in accordance with a higher expression of PPAR-γ, an important marker of adipogenesis, by western blotting assay (Fig. 1E).

MSCs, the promising source for cytotherapy, possess not only merits including self-renewal and multipotent differentiation, but also profound immunoregulatory properties, which facilitate tissue repair and regeneration [23-26]. To reveal whether endogenous osteoporotic BMMSCs suffer deficient

immunoregulatory capability, we established experimental colitis models and compared the therapeutic effects between sham and OVX BMMSCs. Typical symptoms of inflammatory colitis began to appear in C57B/L mice, including loss of weight, diarrhea and bloody stool, on the fourth day after DSS feeding. The mice in DSS and DSS+PBS groups started to die on the sixth and seventh days, and the survival rate sharply decreased to zero on the eighth day (Fig. 2A). Appearance and histological analysis of colons confirmed that DSS feeding caused severe inflammation and damage to colon mucosa (Fig. 2D-E). Sham BMMSCs injected intravenously significantly alleviated DSS-induced body weight loss (Fig. 2B), disease activity index (Fig. 2C), and histological colon inflammation and damage (Fig. 2E), while improving survival rate and colon length (Fig. 2A, D). However, administration of OVX BMMSCs exerted deficient immuno-regulatory effects on the same disease model (Fig. 2A-E). Taken together, these results indicated that the regenerative capabilities of endogenous BMMSCs including lineage differentiation balance and immuno-modulatory properties were significantly impaired in OVX mice.

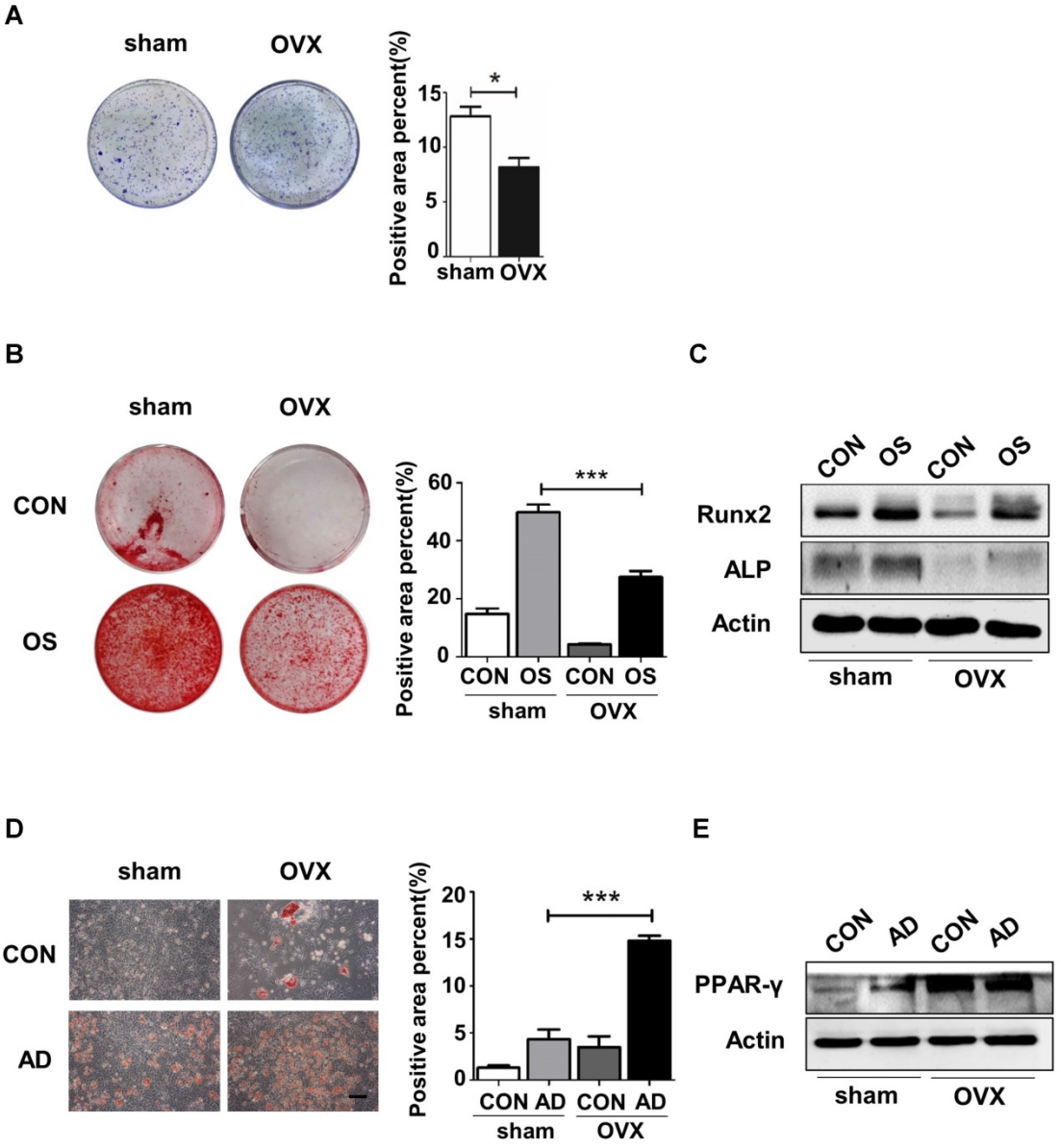

Figure 1. OVX BMMSCs manifested decreased self-renewal and osteogenic differentiation but increased adipogenic differentiation. (A) 5×10^2 primary BMMSCs from sham and OVX model were separately seeded in 5 cm plastic plates and cultured for 10 days. CFU-F was stained with crystal-violet and colony rate was measured (n=3). (B) 2×10^5 sham and OVX BMMSCs at passage one (P1) were separately seeded in 12-well plates and underwent osteogenic induction for 14 days. Mineralized nodules were detected by Alizarin Red staining and quantified to corresponding parameters of mineralized area over total area (n=3). (C) 4×10^5 P1 sham and OVX cells were separately seeded in 6-well plates and induced with osteogenic differentiation medium for 7 days. Western blotting analysis detected the protein expressions of Runx2 and ALP, with Actin as the internal control (n=3). (D) Sham and OVX BMMSCs were seeded in 12-well plates and induced with adipogenic medium for 7 days. Lipid droplets were stained by Oil Red O and quantified to corresponding parameters of lipid droplets area over total area (n=3). (E) Sham and OVX cells were separately induced with adipogenic differentiation medium. Western blotting analysis detected the PPAR-γ protein expression after 5 days of adipogenic induction, with Actin as loading control(n=3). Scale bar, 100 μm. Data are shown as mean ± SD, *P < 0.05, **P < 0.01, ***P < 0.001.

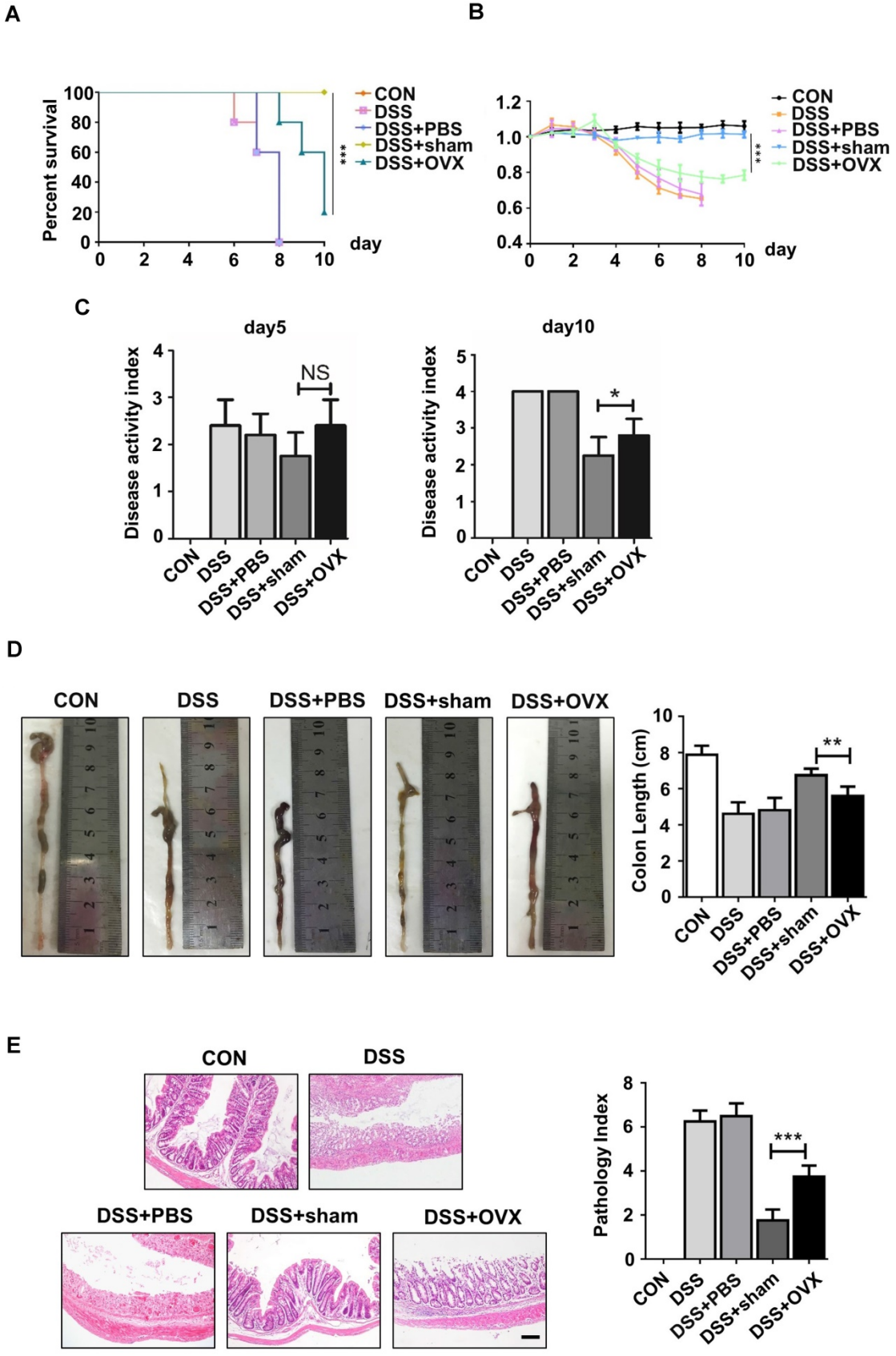

Figure 2. OVX BMMSCs also exhibited declined immuno-regulatory capacity in treating DSS-induced mice model. (A) Survival rates were recorded daily for 10 days (n=5). (B) The relative changes of body weight were calculated as daily body weight divided by initial body weight for 10 days (n=5). (C) Disease activity index (DAI) was determined on day 5 and day 10 according to the symptoms of colitis (n=5). (D) Colon length was measured on day 10 after sacrifice (n=5). (E) H&E staining was conducted to determine the histological changes of isolated colon after sacrifice (n=5). The pathological index of each colon was evaluated and presented in column (n=5). Scale bar, 200 μm. Data are shown as mean ± SD, *P < 0.05, **P < 0.01, ***P < 0.001.

Autophagy decreased in both osteoporotic BMMSCs and bone marrow

Autophagy is a conserved physical process of lysosomal degradation that is essential for cell survival, differentiation, development, and homeostasis [13]. Recent studies revealed that autophagy plays a role in cellular differentiation such as mitochondrial clearance during erythrocyte differentiation or fat droplet deposition during adipocyte differentiation [27]. To investigate whether the malfunctional differentiation of OVX BMMSCs is associated with autophagy, we compared autophagy activity in sham and OVX BMMSCs. We measured the expression of Beclin1 and LC3, which participate in the initiation, expansion and phagopore formation of autophagy [28], and P62, an index of autophagic degradation [29]. Western blotting showed reduction of Beclin1 and LC3 and accumulation of P62 in OVX BMMSCs compared with sham BMMSCs (Fig. 3A). In addition, their difference in autophagy activity was confirmed by quantitative PCR, through detecting mRNA expression levels of ATG genes (BECN1, LC3 and P62) (Fig. 3B). Fluorescence microscopy of OVX BMMSCs cells stained with LC3 showed fewer dotted cytoplasmic structures, compared to sham BMMSCs (Fig. 3C), and the difference was supported by TEM assay (Fig. 3D). All the tests above indicated that the autophagy level decreased in osteoporotic BMMSCs. To explore the role of autophagy in bone metabolism, we further detected autophagy activity of Sca-1$^+$ cells in the femur of sham and OVX mice. Fluorescence microscopy of OVX mouse femur showed less percentage of LC3$^+$ cells in Sca-1$^+$ cells (Fig. 3E), which was consistent with fewer and atypical autophagosomes in OVX mouse femur under TEM (Fig. 3F).

Autophagy is required to maintain the lineage differentiation of BMMSCs

Initially, we explored whether the lineage commitment of BMMSCs is disturbed by autophagy. The administration of rapamycin, a classical inhibitor of mTOR (Mammalian Target of rapamycin), which is upstream and inhibits autophagy, rescued autophagy in OVX BMMSCs at a concentration of 100 nM. Western blotting assay revealed increased Beclin1 and LC3 protein and reduced p62 expression in rapamycin-treated OVX BMMSCs (Fig. S3). To mimic the deficient autophagy activity and investigate whether autophagy affects the lineage commitment of BMMSCs, shRNA was used to silence BECN1 and ATG5 in sham BMMSCs. Efficiency of interference was confirmed by western blotting assay (Fig.S4, A and B). To confirm the role of autophagy in the balance between osteogenic and adipogenic differentiation, we detected osteogenesis of sham BMMSCs, sham BMMSCs+scr-sh, sham BMMSCs+shBECN1, sham BMMSCs+shATG5, OVX BMMSCs and OVX BMMSCs+rapamycin. Alizarin Red staining confirmed that osteogenic differentiation decreased in sham BMMSCs with suppressed autophagy, while it increased in OVX BMMSCs with activated autophagy (Fig. 4A). Protein expressions of Runx2 and ALP revealed the role of autophagy in regulating osteogenesis of BMMSCs (Fig. 4C). Moreover, Oil Red O staining showed that the number of lipid droplets grew in autophagy-depressed sham BMMSCs and declined in autophagy-promoted OVX BMMSCs (Fig. 4B). Protein PPAR-γ was upregulated in sham BMMSCs with reduced autophagy level but downregulated in OVX BMMSCs with restored autophagy (Fig. 4D). Taken together, the results indicated that autophagy participates in the lineage differentiation of BMMSCs, and activation of autophagy could rescue osteogenesis in OVX BMMSCs.

Considering the balance between osteogenesis and osteoclastogenesis is vital in bone homeostasis, we also explored whether autophagy in BMMSCs functions in modulating differentiation and maturation of preosteoclast. Previous reports have revealed the role of OPG/RANKL in the communications between BMMSCs, osteoblasts and osteoclasts [30]. BMMSCs participate in bone resorption by secreting OPG/RANKL to regulate preosteoclast differentiation and activation [31]. Therefore, we investigated whether autophagy affects OPG and RANKL expression on BMMSCs. BMMSCs were administrated with scr-sh/shBECN1/shATG5 and rapamycin. Western blotting demonstrated that RANKL expression reduced in BMMSCs with suppressed autophagy. On the contrary, expression of OPG was upregulated in BMMSCs administrated with rapamycin (Fig.4E). Moreover, OPG/RANKL ratio was calculated through quantifying secretory OPG and RANKL in conditioned culture medium by ELISA kit (Fig. 4F), which revealed autophagy influences the OPG/RANKL secreted by BMMSCs. Taking together, autophagy activity effects lineage differentiation and it participates in the BMMSCs' regulation to osteoclasts *in vitro*.

Autophagy maintains the immunoregulatory function of BMMSCs in treating DSS-induced colitis model

Immunoregulation is the central characteristic of BMMSCs in relieving inflammation. As reported, endogenous BMMSCs in an inflammatory microenvironment partly lost their immuno-regulatory capability during OP, which likely further

deteriorated the inflammation progress. Considering restoration of autophagy partly reversed abnormal lineage commitment in OVX BMMSCs, we wondered whether immuno-regulatory capability is influenced by autophagy. Experimental colitis mice were subjected to intravenous injection with sham BMMSCs, sham BMMSCs+scr-sh, sham BMMSCs+shBECN1, sham BMMSCs+shATG5, OVX BMMSCs and OVX BMMSCs+rapamycin. Mortality was recorded daily and survival rate differences among groups demonstrated that sham BMMSCs were the most efficient cells in alleviating DSS-induced colitis. However, the ability was weakened when BECN1 or ATG5 was suppressed. Meanwhile, improvement was noticed in OVX BMMSCs+rapamycin (Fig. 5A). Body weight loss and severity of colon inflammation were affected by BMMSCs with interfered autophagy level, suggesting that autophagy promoted the immuno-therapy of OVX BMMSCs (Fig. 5B-C). Colons were resected after sacrifice on day 10. The length and appearance of colon indicated alleviated colitis in the mice injected with OVX BMMSCs with restored autophagy level, showing less hemorrhage and looser stools (Fig. 5D-E). Moreover, H&E staining further showed that the structure of intestinal mucosa was recovered through the BMMSCs with activated autophagy (Fig. 5F). The data above revealed the vital function of autophagy in maintaining the immuno-regulatory property of BMMSCs.

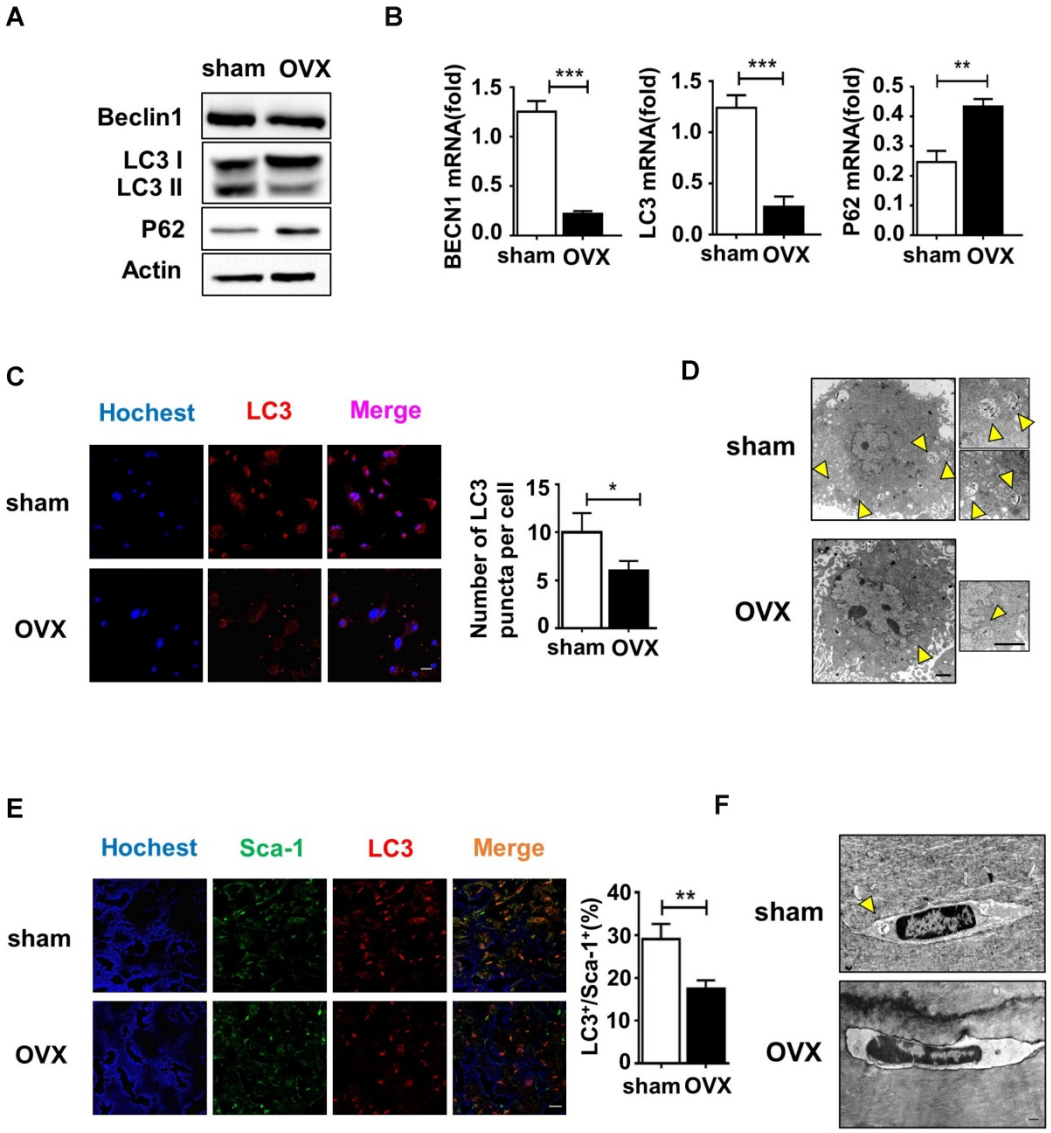

Figure 3. Autophagy level decreased significantly in both OVX BMMSCs and bone marrow. (A) Western blotting analysis of autophagy related protein expressions of Beclin1, LC3 and P62 with Actin as loading control (n=3). (B) qRT-PCR was performed to measure relative gene expressions of BECN1, LC3 and P62 (n=3). (C) The distribution of autophagosomes in BMMSCs were visualized by LC3 immunofluorescent staining (red). Merged image confirmed the presence of LC3 co-expression with the blue nucleus (n=3). Scale bar, 20 μm. (D) The representative morphology of autophagic vacuoles as autophagosomes was observed by TEM. Yellow arrows indicate the autophagosomes in BMMSCs (n=3). Scale bar, 2 μm. (E) Immunofluorescence detected the co-expression of Sca-1 (green) and LC3 (red) in BMMSCs with blue nucleus in bone marrow (n=3). Scale bar, 50 μm. (F) TEM (×8000) micrographs of autophagosomes in bone marrow cells. The yellow arrow indicates the autophagosome (n=3). Scale bar, 2 μm. All the analyses were performed in BMMSCs or femur bone marrow of sham and OVX mice. Data are shown as mean ± SD, *P < 0.05, **P < 0.01, ***P < 0.001.

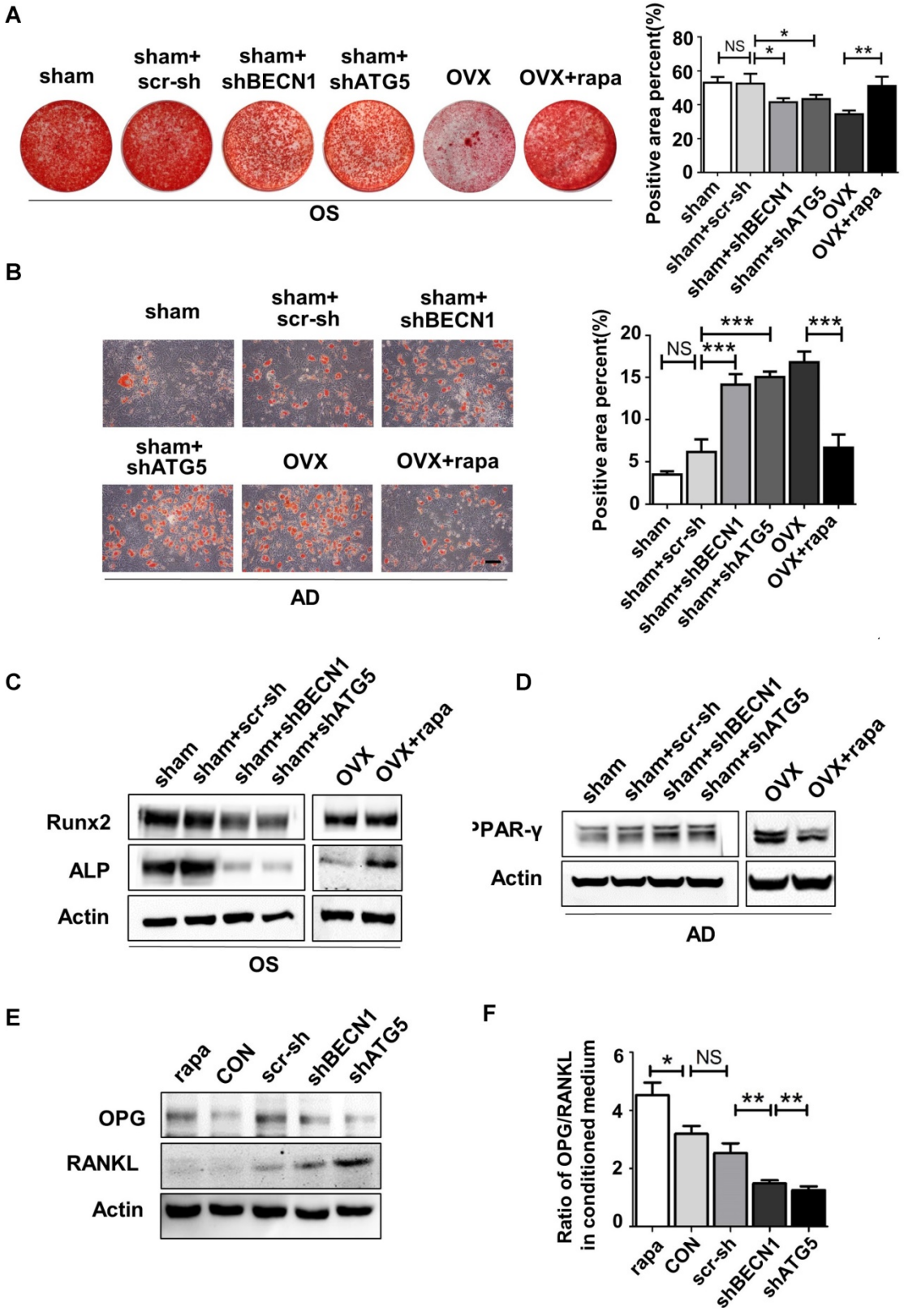

Figure 4. Autophagy maintained the lineage differentiation capability of BMMSCs. (A) Alizarin Red staining was performed to detect mineralized nodules formed in sham BMMSCs, sham BMMSCs+scr-sh, sham BMMSCs+shBECN1, sham BMMSCs +shATG5, OVX BMMSCs and OVX BMMSCs +rapamycin 14 days after osteogenic induction. Corresponding parameters of mineralized area over total area were quantified (n=3). (B) Lipid droplet formation was detected by Oil Red O staining 7 days after adipogenic induction with positive area quantified (n=3). (C) Protein expressions of Runx2, ALP and Actin in sham BMMSCs, sham BMMSCs+scr-sh, sham BMMSCs+shBECN1, sham BMMSCs +shATG5, OVX BMMSCs and OVX BMMSCs +rapamycin were measured through western blotting (n=3). (D) Expressions of PPAR-γ and Actin were tested in sham BMMSCs, sham BMMSCs+scr-sh, sham BMMSCs+shBECN1, sham BMMSCs +shATG5, OVX BMMSCs and OVX BMMSCs +rapamycin (n=3). (E) Expressions of OPG and RANKL were measured in BMMSCs, BMMSCs+scr-sh, BMMSCs+shBECN1, BMMSCs+shATG5, and BMMSCs+rapamycin by western blotting (n=3). (F) Secretory OPG and RANKL expressions in conditioned medium of BMMSCs, BMMSCs+scr-sh, BMMSCs+shBECN1, BMMSCs+shATG5, BMMSCs+rapamycin were detected by ELISA kit and the ratio of OPG/RANKL was calculated (n=3). Scale bar, 100 μm. Data are shown as mean ± SD, *P < 0.05, **P < 0.01, ***P < 0.001.

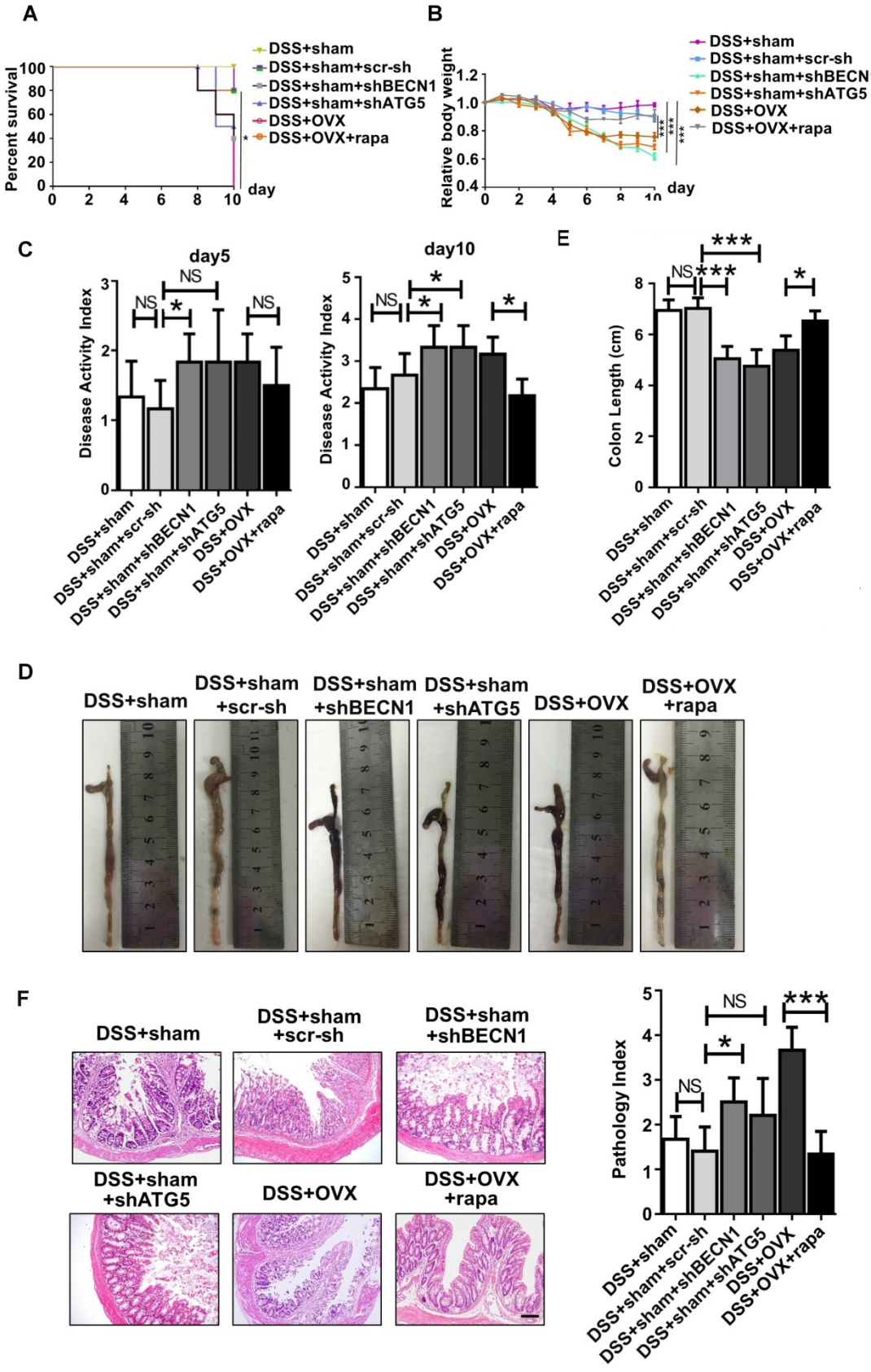

Figure 5. Autophagy maintained the immuno-regulatory function of BMMSCs. (A) Survival rates were recorded daily for 10 days for experimental colitis mice injected with sham BMMSCs, sham BMMSCs+scr-sh, sham BMMSCs+shBECN1, sham BMMSCs+shATG5, OVX BMMSCs and OVX BMMSCs+rapamycin (n=5). (B) The relative changes of body weight were calculated as daily body weight divided by initial body weight for 10 days (n=5). (C) Disease activity index (DAI) was determined on day 5 and day 10 according to the symptoms of colitis (n=5). (D and E) Colon length was measured on day 10, after sacrifice (n=5). (F) H&E staining was conducted to detect the histological changes of isolated colon after sacrifice (n=5). The pathological index of each colon was evaluated and presented (n=5). Scale bar, 200 μm. Data are shown as mean ± SD, *P < 0.05, **P < 0.01, ***P < 0.001.

Rapamycin rescues the regenerative properties of endogenous BMMSCs and attenuates the osteoporotic phenotype in OVX mice via activating autophagy

We further investigated whether regulation of autophagy could affect the regenerative capability of endogenous BMMSCs and bone mass. Osteoporotic mice were injected with rapamycin intraperitoneally once every two days while the femur of sham mice underwent intra-bone injection with scr-sh virus, shBECN1 virus and shATG5 virus, once every half month. One month later, all mice were sacrificed for tests and analyses.

Micro-CT assay revealed that rapamycin treatment efficiently attenuated bone loss after OVX (Fig. 6A), shown by the increased bone mineral density (BMD), bone volume percentage (BV/TV), trabecular numbers (Tb.N) and trabecular thickness (Tb.Th) (Fig. 6B). Meanwhile, shBECN1 and shATG5 virus treatment had adverse effects on bone mass, resulting in decreased related indices (Fig. 6A-B). Moreover, we performed calcein labeling analysis on femur and found higher osteogenesis rate in rapamycin-treated osteoporotic mice (Fig. 6C). To evaluate adipogenesis, we also carried out Oil Red O staining (Fig. 6D) and observed decreased lipid droplets in bone marrow of OVX mice with rapamycin administration.

We also harvested BMMSCs from six groups, including sham mice (sham), sham mice with intra-bone injection of scr-sh virus (sham+scr-sh), sham mice with intra-bone injection of shBECN1 virus(sham+shBECN1), sham mice with intra-bone injection of shATG5 virus (sham+shATG5), OVX mice (OVX), and OVX mice with intraperitoneal injection of rapamycin (OVX+rapamycin). The cells were cultured and exposed to osteogenic/adipogenic induction to determine the differentiation ability of endogenous BMMSCs from the groups mentioned above. According to the results, Alizarin Red staining showed more mineralized nodules in BMMSCs from rapamycin treatment mice and less osteogenesis in cells from mice with administration of shBECN1 and shATG5 virus (Fig. 7A). Decreased lipid droplets in BMMSCs from rapamycin group confirmed that adipogenesis was effectively inhibited. shBECN1 and shATG5 virus triggered over-adipogenesis of endogenous BMMSCs (Fig. 7B). Furthermore, BMMSCs from six groups were harvested and cocultured with T cells to evaluate their immuno-modulatory ability. OVX BMMSCs induced less apoptosis of T cells than sham BMMSCs *in vitro*, which is consistent with more serious colitis symptoms in the mice injected with OVX BMMSCs. Meanwhile, BMMSCs from autophagy-suppressed mice (shBECN1 and shATG5) triggered less apoptosis of T cells, while BMMSCs from rapamycin-treated OVX mice showed restored capability in regulating T cells apoptosis (Fig. 7C). Taken together, recover of autophagy could restore lineage commitment and immunotherapeutic property of OVX BMMSCs and alleviate osteoporotic phenotype in mice.

Discussion

During the past two decades, pharmacologic therapy for OP focuses on depressor of bone resorption and activators of bone formation [32]. Currently available strong agents are bisphosphonates, which trigger osteoclast apoptosis [33], and denosumab, an anti-RANKL antibody [34]. However, the effect of bisphosphonates reaches a bottleneck around 3 to 5 years later. In addition, using bisphosphonates in long term has been reported to be associated with atypical femoral fractures [35]. For denosumab, it is reported to be associated with atypical femoral fractures and osteonecrosis of the jaw. In addition, discontinuation of it causes a rapid increase in bone remodeling, resulting in a rapid loss of bone and increased risk of fractures [36]. PTH, the promising pure anabolic agent, stimulates bone formation via binding to its type 1 receptor (PTH1R) on the surface of osteoblasts and osteocytes. However, PTH shows a restricted anabolic window of no more than 2 years [37]. Moreover, teriparatide, the PTH analog and the most effective agent for osteoporosis treatment, leads to adverse effects on bone resorption [38]. Additionally, side effects of PTH include nausea, headache and dizziness. Transient hypercalcemia and hypercalciuria induced by PTH 1–84 have been reported [37].

According to reports in recent years, OP is not only characterized by an imbalance of remodeling between bone resorption and bone formation, but is also associated with a decrease in bone mass but high adiposity in the bone marrow cavity [39, 40]. The abnormal lineage commitment of BMMSCs is closely related to the bone loss and fat accumulation in bone marrow during OP. In addition, postmenopausal OP is regarded as cytokine pattern-mediated inflammation [41] and increasing *in vivo* inflammatory factors may affect the immunosuppressive ability of BMMSCs (according to unpublished data in our lab). In this study, we noticed lower autophagy activity in BMMSCs and bone marrow of OVX mice. Furthermore, the impaired lineage differentiation and immunoregulatory capability could be partly corrected through activation of autophagy in osteoporotic BMMSCs.

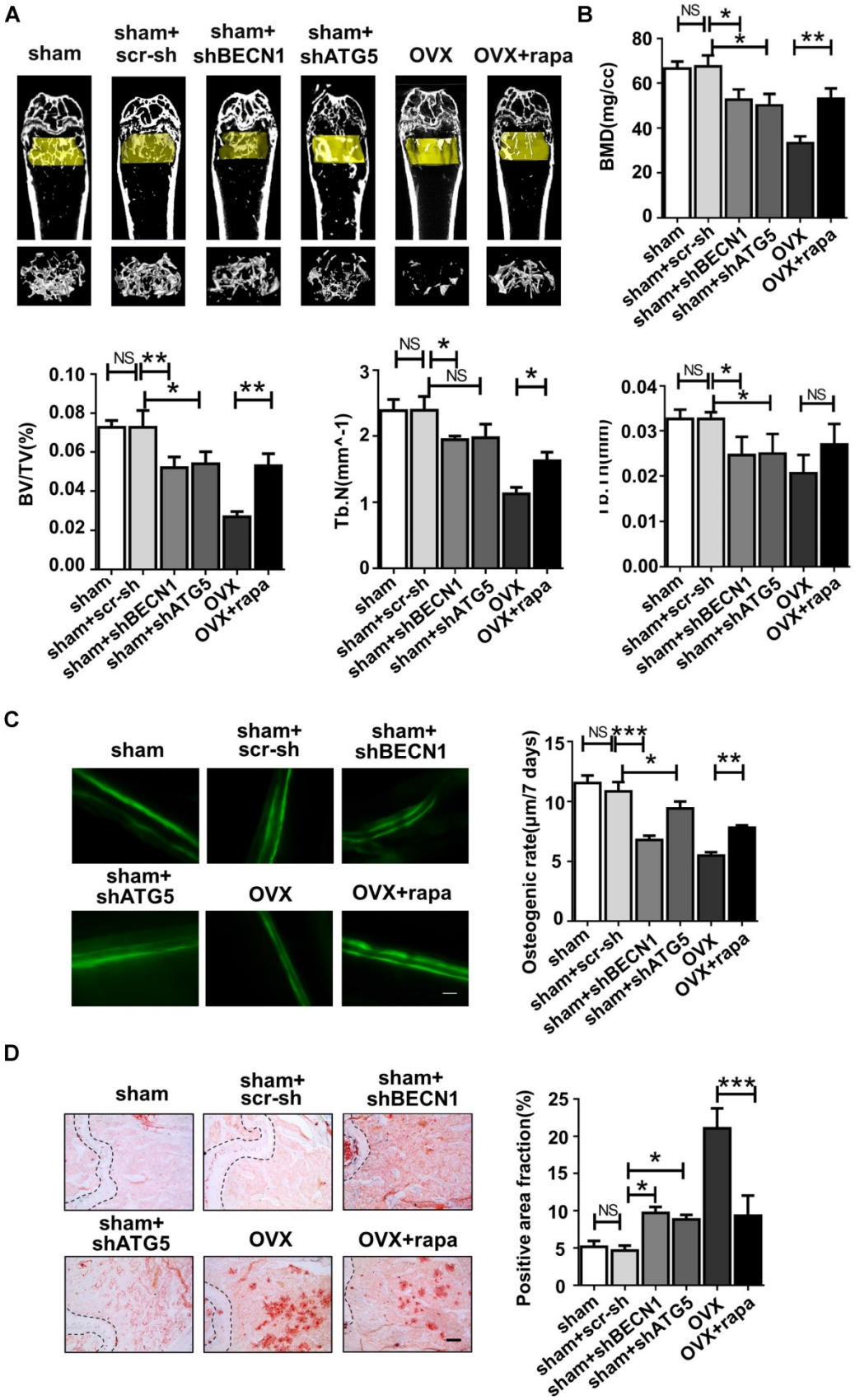

Figure 6. Autophagy level controls the skeletal phenotype in mice. Mice of six groups described above were sacrificed after treatment. Distal parts of femurs were subjected to (A) micro-CT to quantify (B) Bone mineral density (BMD), bone volume/total volume (BV/TV), trabecular bone number (Tb.N) and trabecular thickness (Tb.Th) (n=5). (C) Calcein labeling in distal part of femurs was observed under fluorescence microscope. Distance between two fluorescent strips was measured with Image pro software (n=5). Scale bar, 100 μm. (D) Bone marrow cavity were stained with Oil Red O to calculate the percentage of adipocytes in areas under growth plates of distal femur (n=5). Scale bar, 200 μm. Data are shown as mean ± SD, *P < 0.05, **P < 0.01, ***P < 0.001.

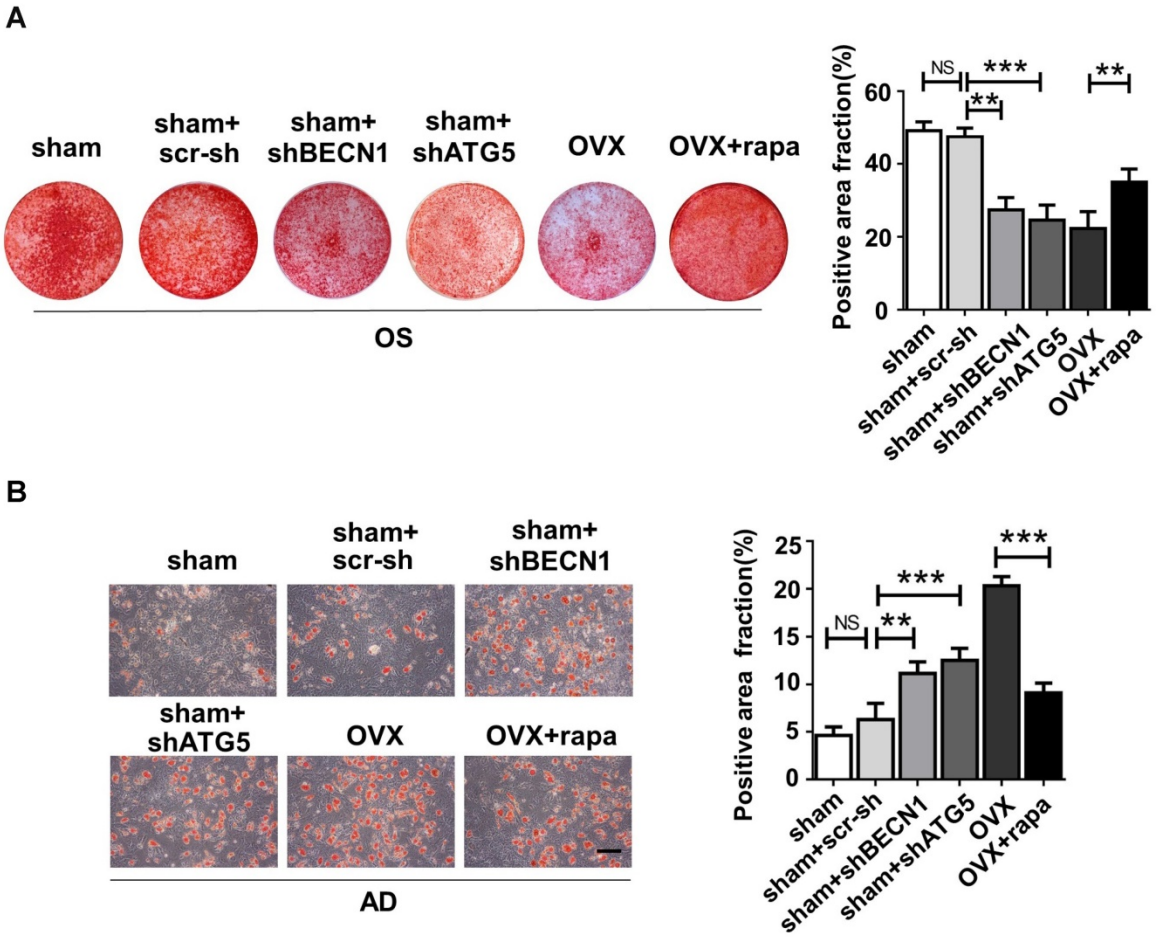

Figure 7. Autophagy regulates the lineage differentiation and Immuno-modulatory capability of endogenous BMMSCs. BMMSCs were harvested from sham mice, sham mice+scr-sh, sham mice+shBECN1, sham mice+shATG5, OVX mice and OVX mice+rapamycin. (A) Cells were stained by Alizarin Red after 14-day osteogenic induction (n=3). (B) Oil Red O staining was performed to detect lipid droplets formation 7 days after adipogenic induction (n=3). Scale bar, 100 μm. (C) Dot plot of FITC-Annexin V (x axis)/PI (y axis) in T cells cocultured with BMMSCs from six groups. Data are shown as mean ± SD, *P < 0.05, **P < 0.01, ***P < 0.001.

Autophagy functions to degrade and recycle damaged and/or aging proteins and organelles for cell homeostasis. In the recent decades, autophagy has been gradually deemed as a crucial process taking part in the self-renewal, pluripotency, development, differentiation and quiescence of stem cells [42, 43]. It has been reported impairment of this process is associated with the pathogenesis of various diseases, such as cancer, neurodegeneration, infection and aging [11]. Autophagy process is noticed to be involved in differentiations of cells. For example, constitutive levels of autophagy were observed in embryonic stem cells, and an upregulation of autophagy proteins occurs early during differentiation. Besides, it has been shown that the reprogramming of somatic cells into induced pluripotent stem cells involves the process and signaling pathways of autophagy [44-46]. However, the role of autophagy in MSCs is largely unknown [47, 48]. Though the number of studies on MSC autophagy is limited, significant constitutive levels of autophagy-associated proteins upregulated in these cells have been shown, with potential early activation and loss of phenotype later during differentiation [48, 49], suggesting that there is probably an underlying function of autophagy in the differentiation of MSCs and maintenance of stem cells. Moreover, the role of autophagy in the immunosuppressive property of MSCs has been reported [50]. All the findings remind us of the possibility of autophagy in maintaining the regenerative properties of MSCs.

The difference in colony-forming units between sham and OVX BMMSCs demonstrated deficient self-renewal in the latter cells. Next, lineage differentiation commitment of OVX BMMSCs was evaluated by detecting the protein expressions of osteogenic and adipogenic differentiation markers. Runx2 and PPARγ are generally regarded as the master regulators of osteogenesis and adipogenesis [51]. Runx2 is one of the most crucial transcription factors for early osteoblast differentiation [52], and it triggers ALP expression by binding to the ALP promoter region, which is crucial in calcification of bone matrix [53, 54]. PPARγ is generally considered as the master regulator of adipogenesis, and it also has well-described anti-osteoblastogenic effects. As shown in Fig. 1, the skewing to adiposity was reconfirmed in the BMMSCs of OP models established in our study by the distinguished extent of mineralized nodules and lipid droplet formation. MSCs, significant sources of tissue regeneration, are mainly dependent on characters such as self-renewal, multipotency and immunoregulation. Hence, we performed an experimental colitis model to further investigate the immunotherapeutic capability of OVX BMMSCs. As shown, cells were unable to obviously attenuate symptoms and pathological damage of intestinal mucosa, implying that the BMMSCs from the inflammatory microenvironment may have lost their immunoregulatory property in maintaining homeostasis. In sum, regenerative properties of BMMSCs are impaired during OP.

We focused on autophagy to find out the potential mechanism responsible for the impaired regenerative properties in OVX BMMSCs and observed less protein expression of Becin1, decreased ratio of LC3II/LC3I and accumulated P62 in OVX BMMSCs. Beclin-1 is an important constituent of the class III PI3K (Phosphatidylinositide 3-kinases) complex, and is involved in the initiation of autophagosome formation. LC3 is present in free cytoplasmic form as LC3I. It produces the LC3II form when conjugated to phosphatidylethanolamine in the membrane of an autophagosome. Therefore, LC3II is a useful marker of autophagic vacuoles and both LC3I and LC3II are key standards in monitoring autophagy level [55]. P62 serves as an index of autophagic degradation. In addition, reductions in BECN1 and LC3 mRNA and increases in P62 mRNA were also noticed, implying autophagy was impaired during transcription in OVX BMMSCs.

It has been verified that pro-inflammatory cytokines (tumor necrosis factor-α, interleukin-1, and interleukin-6) and reactive oxygen species increase during menopause in mice and women suffering withdrawal of estrogen (e.g., OP) [56, 57]. TNF-α plays a central role in the pathogenesis of postmenopausal OP through affecting commitment and differentiation of BMMSCs [58, 59]. A previous study showed that the expression of LC3 decreased and that of p62 increased in the PDLSCs subjected to TNF-α for 7 days [60]. Furthermore, in retinal pigmented epithelial (RPE) cells, acute oxidative stress induced a marked increase in autophagy, whereas under chronic oxidative stress, autophagy was reduced [61]. Thereby, there may be negative effects of inflammatory microenvironment, particularly chronic inflammation, on the autophagy in BMMSCs during OP.

Considering estrogen withdrawal during post menopause, to find out the effect of estrogen on autophagy activity, BMMSCs were administrated with a range of estrogen concentrations from 0.1 to 10^3 nM [28, 29]. The Beclin1 and LC3 showed stable expressions at different concentrations, while P62 seemed to accumulate with increasing estrogen dosage (Fig. S5). The inconsistent alteration of proteins could not be reasonably explained through autophagy because P62 does not exclusively participate in the autophagic progress, but also

functions in other autophagy-independent ways [62]. Thus, we considered that autophagy was not influenced by estrogen in BMMSCs.

In order to explore whether impaired autophagy is associated with abnormal lineage differentiation of OVX BMMSCs, we initially adopted rapamycin, a specific inhibitor of mTOR, as autophagy activator [63]. Rapamycin has a broad-spectrum effect on cell growth through targeting mTOR, which promotes cell growth by stimulating *de novo* synthesis of primary building blocks, such as proteins, nucleotides and lipids [64]. It cannot be ignored that mTORC1 enhances lipogenesis by activating SREBPs and thereby mediates the anti-adipogenesis effect of rapamycin [65]. To rule out this disturbance from the administration of rapamycin, BECN11 and ATG5 were silenced in sham BMMSCs. As results show, inhibition of autophagy by shBECN1 and shATG5 exerted opposite effects to rapamycin *in vitro,* implying that autophagy level indeed modulates BMMSC lineage differentiation. We proceeded to investigate the role of autophagy in the immunotherapeutic properties of BMMSCs through a DSS-induced colitis model, which is the most widely used model resembling acute or chronic colitis [66] and is featured by severe local inflammation in intestinal mucosa [67]. Data support autophagy as a key role in sustaining immunoregulatory capacity in BMMSCs.

Finally, we turned to the treatment of OP with the expectation to rescue BMMSCs' regenerative characteristics through activating autophagy in OVX mice *in vivo*. We are obliged to admit the weakness of rapamycin, considering the non-specific effect of systemic administration of rapamycin on bone mass. This is because rapamycin is not a specific autophagy activator and has broad-spectrum effects on various cells *in vivo*. Thus, intra-bone injection of shBECN1 and shATG5 were adopted to rule out possible autophagy-independent effects brought on by rapamycin. The BMMSCs harvested one month later obviously presented restored lineage differentiation after rapamycin treatment. Inversely, shBECN1 and shATG5 impaired osteogenesis and facilitated adipogenesis of endogenous BMMSCs in sham mice. Furthermore, attenuation of bone loss, augmentation of bone formation and reduction of lipid droplets in bone marrow coincided with lineage shift of BMMSCs in osteoporotic mice. To explore whether autophagy influences the apoptosis of BMMSCs, we performed Annexin V/ PI staining on sham BMMSCs, sham BMMSCs+scr-sh, sham BMMSCs+shBECN1, sham BMMSCs+shATG5, OVX BMMSCs and OVX BMMSCs+rapamycin (Fig. S6). As shown, the apoptosis slightly increased in BMMSCs with suppressed autophagy and mildly decreased in OVX BMMSCs administrated with rapamycin. The change of apoptosis induced by interfered autophagy was too subtle to affect numbers of BMMSCs in vitro, which suggested that restoration of bone mass probably attributed to BMMSCs with recovered function rather than more BMMSCs in osteoporotic mice. These results remind us of the possible function of autophagy in modulating BMMSCs and subsequent effect on bone mass, and thus should be further studied.

Given that osteoclasts play an important role in bone remodeling via bone resorption, we retrospected previous studies and concluded the role of autophagy in regulating the function and activity of osteoclasts. Inhibition of autophagy decreased TRAP and CTSK gene expressions in osteoclasts [68]. Absence of Atg7 suppressed the conversion of LC3I to LC3II and impaired the resorptive ability of osteoclasts; There is a much higher chance that Atg5-deficient osteoclasts lack a normal ruffled border [69]. Suppression of NF-κB-dependent autophagy is important to isoliquiritigenin-mediated anti-osteoclastogenesis [70]. However, in another study, PBMC osteoclast precursors in critically ill patients' blood showed suppressed autophagy-related makers. In comparison with healthy control PBMCs, abnormal osteoclastogenesis was markedly decreased in patient PBMC by promotion of autophagy with mTOR inhibitor rapamycin. This supports the assumption that the extreme osteoclast formation in critical ill patients largely involves deficient autophagy [71]. As the above reports described, autophagy activation may affect maturation and/or resorptive functions of osteoclasts. In this research, we mainly focus on the role of autophagy in aberrant BMMSCs from OVX mice because the lineage differentiation of BMMSCs is crucial in the balance between osteogenesis and adipogenesis, which is an important perspective in exploring pathogenesis of OP. We did not pay attention to osteoclasts, not because aberrant bone resorption in OP condition is overlooked, but because it is not the focus in this work. The effects of rapamycin and autophagy on osteoclastogenesis in the OVX model should be paid more attention in future studies. Even so, we observed the relation between autophagy and BMMSCs' regulatory capability on osteoclasts.

Previous studies mainly focused on the role of autophagy in osteoblasts, osteocytes and osteoclasts, which are almost terminally differentiated cells in the skeletal system. Here, we investigated the mechanism in OP of the imbalance between osteogenesis and adipogenesis as well as BMMSCs' multipotent differentiation capability (especially osteogenic and

adipogenic differentiation), which enables them to maintain bone homeostasis. In our research, the correlation between impaired autophagy and abnormal lineage differentiation was established in BMMSCs, which may imply the role of autophagy in maintaining BMMSCs' function in physiological status.

There are still some questions that need to be further investigated. For example, rapamycin, an immuno-suppressive drug, is used extensively to prevent graft rejection in transplant patients; however, previous studies revealed that rapamycin severely weakens human adipocyte differentiation of subcutaneous pre-adipocytes *in vitro* [72] and prevents accretion in body weight of mice fed high-fat diets via reducing lipid accumulation [73]. These findings revealed the negative effect of rapamycin on lipid metabolism and may be partly associated with lower adipogenesis in bone marrow. Thus, we need to further rule out this interference from the anti-adipogenesis effect of rapamycin. In addition, potential pathways that are involved in the autophagic function in lineage differentiation and immunotherapy of BMMSCs, are worth further investigation.

Conclusion

Here, we showed that the osteoporotic BMMSCs manifested impaired osteo/adipogenic differentiation and inhibited immunotherapeutic properties, which were caused by decreased autophagy. Specifically, we investigated that autophagy was required to maintain the function of BMMSCs, including differentiation and immunoregulation. Rapamycin treatment rescued the function of endogenous BMMSCs and alleviated osteoporotic phenotype via reactivating autophagy in OVX mice. Thus, we infer that autophagy in BMMSCs may become a new and effective therapeutic target for OP.

Abbreviations

OP: osteoporosis; MSCs: mesenchymal stem cells; BMMSCs: bone marrow mesenchymal stem cells; OVX: ovariectomy; ALP: alkaline phosphatase; RUNX2: runt-related transcription factor 2; PPAR-γ: peroxisome proliferator-activated receptor gamma; OPG: osteoprotegerin; RANKL: receptor activator of NF-kB ligand; DSS: dextran sulfate sodium; LC3: microtubule-associated protein 1 light chain 3; H&E: hematoxylin and eosin; shRNA: short hairpin RNA; TEM: transmission electron microscope; ELISA: enzyme-linked immunosorbent assay; FBS: fetal bovine serum; BMD: bone mineral density; BV/TV: bone volume/total volume; Tb.N: trabecular bone number; Tb.Th: trabecular thickness.

Acknowledgments

We appreciate Hua Ni, Xiaolin Xu, Jiangtao Guan, Shuli Cheng, Bingyi Shao and Yang Yu for technical assistance of cell culture and animal experiment in the Research and Development Center for Tissue Engineering, Fourth Military Medical University, Xi'an, Shaanxi, China.

Funding

This study was supported and sponsored by grants from the National Natural Science Foundation (NNSF) of China (31571532, 81371155 and 31570991) and the Nature Science Foundation of China (81620108007).

Author contributions

Yan Jin, Wenjia Liu, conceived and designed the research. Yan Jin and Wenjia Liu supervised the project. Meng Qi, Liqiang Zhang and Yang Ma performed the experiments, analyzed the data. Meng Qi wrote the manuscript. Yan Jin, Wenjia Liu reviewed the manuscript. Yang Ma, Yi Shuai, Liya Li, Kefu Luo and Shuli Cheng participated in animal model establishment and sample collection of partial animal experiments

Supplementary Material

Supplementary figures.
http://www.thno.org/v07p4498s1.pdf

Competing Interests

The authors have declared that no competing interest exists.

References

1. Cooper C, Campion G, Melton LJ, 3rd. Hip fractures in the elderly: a world-wide projection. Osteoporos Int. 1992; 2: 285-9.
2. Liu Y, Wu J, Zhu Y, Han J. Therapeutic application of mesenchymal stem cells in bone and joint diseases. Clin Exp Med. 2014; 14: 13-24.
3. Tabatabaei-Malazy O, Salari P, Khashayar P, Larijani B. New horizons in treatment of osteoporosis. Daru. 2017; 25: 2.
4. Rizzoli R, Bischoff-Ferrari H, Dawson-Hughes B, Weaver C. Nutrition and bone health in women after the menopause. Womens Health (Lond). 2014; 10: 599-608.
5. Liu Y, Yang R, Liu X, Zhou Y, Qu C, Kikuiri T, et al. Hydrogen sulfide maintains mesenchymal stem cell function and bone homeostasis via regulation of Ca(2+) channel sulfhydration. Cell Stem Cell. 2014; 15: 66-78.
6. Turgeman G, Zilberman Y, Zhou S, Kelly P, Moutsatsos IK, Kharode YP, et al. Systemically administered rhBMP-2 promotes MSC activity and reverses bone and cartilage loss in osteopenic mice. J Cell Biochem. 2002; 86: 461-74.
7. Yang N, Wang G, Hu C, Shi Y, Liao L, Shi S, et al. Tumor necrosis factor alpha suppresses the mesenchymal stem cell osteogenesis promoter miR-21 in estrogen deficiency-induced osteoporosis. J Bone Miner Res. 2013; 28: 559-73.
8. Rodriguez JP, Montecinos L, Rios S, Reyes P, Martinez J. Mesenchymal stem cells from osteoporotic patients produce a type I collagen-deficient extracellular matrix favoring adipogenic differentiation. J Cell Biochem. 2000; 79: 557-65.
9. Zhang ZM, Jiang LS, Jiang SD, Dai LY. Osteogenic potential and responsiveness to leptin of mesenchymal stem cells between

postmenopausal women with osteoarthritis and osteoporosis. J Orthop Res. 2009; 27: 1067-73.
10. Rosen CJ, Bouxsein ML. Mechanisms of disease: is osteoporosis the obesity of bone? Nat Clin Pract Rheumatol. 2006; 2: 35-43.
11. Mizushima N, Levine B, Cuervo AM, Klionsky DJ. Autophagy fights disease through cellular self-digestion. Nature. 2008; 451: 1069-75.
12. Mizushima N. Autophagy: process and function. Genes Dev. 2007; 21: 2861-73.
13. Levine B, Kroemer G. Autophagy in the pathogenesis of disease. Cell. 2008; 132: 27-42.
14. Nollet M, Santucci-Darmanin S, Breuil V, Al-Sahlanee R, Cros C, Topi M, et al. Autophagy in osteoblasts is involved in mineralization and bone homeostasis. Autophagy. 2014; 10: 1965-77.
15. Liu F, Fang F, Yuan H, Yang D, Chen Y, Williams L, et al. Suppression of autophagy by FIP200 deletion leads to osteopenia in mice through the inhibition of osteoblast terminal differentiation. J Bone Miner Res. 2013; 28: 2414-30.
16. Zhang L, Guo YF, Liu YZ, Liu YJ, Xiong DH, Liu XG, et al. Pathway-based genome-wide association analysis identified the importance of regulation-of-autophagy pathway for ultradistal radius BMD. J Bone Miner Res. 2010; 25: 1572-80.
17. Li Q, Liu Y, Sun M. Autophagy and Alzheimer's Disease. Cell Mol Neurobiol. 2017; 37: 377-88.
18. Cheng NT, Meng H, Ma LF, Zhang L, Yu HM, Wang ZZ, et al. Role of autophagy in the progression of osteoarthritis: The autophagy inhibitor, 3-methyladenine, aggravates the severity of experimental osteoarthritis. Int J Mol Med. 2017; 39: 1224-32.
19. Kaarniranta K. Autophagy--hot topic in AMD. Acta Ophthalmol. 2010; 88: 387-8.
20. Fink T, Zachar V. Adipogenic differentiation of human mesenchymal stem cells. Methods Mol Biol. 2011; 698: 243-51.
21. Reseland JE, Syversen U, Bakke I, Qvigstad G, Eide LG, Hjertner O, et al. Leptin is expressed in and secreted from primary cultures of human osteoblasts and promotes bone mineralization. J Bone Miner Res. 2001; 16: 1426-33.
22. Aydin A, Halici Z, Albayrak A, Polat B, Karakus E, Yildirim OS, et al. Treatment with Carnitine Enhances Bone Fracture Healing under Osteoporotic and/or Inflammatory Conditions. Basic Clin Pharmacol Toxicol. 2015; 117: 173-9.
23. Nauta AJ, Fibbe WE. Immunomodulatory properties of mesenchymal stromal cells. Blood. 2007; 110: 3499-506.
24. Le Blanc K, Ringden O. Immunomodulation by mesenchymal stem cells and clinical experience. J Intern Med. 2007; 262: 509-25.
25. Wang D, Niu L, Feng X, Yuan X, Zhao S, Zhang H, et al. Long-term safety of umbilical cord mesenchymal stem cells transplantation for systemic lupus erythematosus: a 6-year follow-up study. Clin Exp Med. 2016.
26. Akiyama K, Chen C, Wang D, Xu X, Qu C, Yamaza T, et al. Mesenchymal-stem-cell-induced immunoregulation involves FAS-ligand-/FAS-mediated T cell apoptosis. Cell Stem Cell. 2012; 10: 544-55.
27. Mizushima N, Levine B. Autophagy in mammalian development and differentiation. Nat Cell Biol. 2010; 12: 823-30.
28. Pierrefite-Carle V, Santucci-Darmanin S, Breuil V, Camuzard O, Carle GF. Autophagy in bone: Self-eating to stay in balance. Ageing Res Rev. 2015; 24: 206-17.
29. Klionsky DJ, Abdelmohsen K, Abe A, Abedin MJ, Abeliovich H, Acevedo Arozena A, et al. Guidelines for the use and interpretation of assays for monitoring autophagy (3rd edition). Autophagy. 2016; 12: 1-222.
30. Silva I, Branco JC. Rank/Rankl/opg: literature review. Acta Reumatol Port. 2011; 36: 209-18.
31. Boyce BF, Xing L. Biology of RANK, RANKL, and osteoprotegerin. Arthritis Res Ther. 2007; 9 Suppl 1: S1.
32. Luigi Gennari SR, Simone Bianciardi, Ranuccio Nuti & Daniela Merlotti. Treatment needs and current options for postmenopausal osteoporosis. Expert Opinion on Pharmacotherapy 2016; 17: 1141-52.
33. Weinstein RS, Roberson PK, Manolagas SC. Giant osteoclast formation and long-term oral bisphosphonate therapy. N Engl J Med. 2009; 360: 53-62.
34. Fukumoto S, Matsumoto T. Recent advances in the management of osteoporosis. F1000Res. 2017; 6: 625.
35. Khosla S, Bilezikian JP, Dempster DW, Lewiecki EM, Miller PD, Neer RM, et al. Benefits and risks of bisphosphonate therapy for osteoporosis. J Clin Endocrinol Metab. 2012; 97: 2272-82.
36. Popp AW, Zysset PK, Lippuner K. Rebound-associated vertebral fractures after discontinuation of denosumab-from clinic and biomechanics. Osteoporos Int. 2016; 27: 1917-21.
37. Gennari L, Rotatori S, Bianciardi S, Nuti R, Merlotti D. Treatment needs and current options for postmenopausal osteoporosis. Expert Opin Pharmacother. 2016; 17: 1141-52.
38. Makras P, Delaroudis S, Anastasilakis AD. Novel therapies for osteoporosis. Metabolism. 2015; 64: 1199-214.
39. Raisz LG. Pathogenesis of osteoporosis: concepts, conflicts, and prospects. The Journal of clinical investigation. 2005; 115: 3318-25.
40. Rachner TD, Khosla S, Hofbauer LC. Osteoporosis: now and the future. Lancet. 2011; 377: 1276-87.
41. Al-Daghri NM, Aziz I, Yakout S, Aljohani NJ, Al-Saleh Y, Amer OE, et al. Inflammation as a contributing factor among postmenopausal Saudi women with osteoporosis. Medicine (Baltimore). 2017; 96: e5780.
42. Rodolfo C, Di Bartolomeo S, Cecconi F. Autophagy in stem and progenitor cells. Cell Mol Life Sci. 2016; 73: 475-96.
43. Levine B. Eating oneself and uninvited guests: autophagy-related pathways in cellular defense. Cell. 2005; 120: 159-62.
44. Tra T, Gong L, Kao LP, Li XL, Grandela C, Devenish RJ, et al. Autophagy in human embryonic stem cells. PloS one. 2011; 6: e27485.
45. Chen T, Shen L, Yu J, Wan H, Guo A, Chen J, et al. Rapamycin and other longevity-promoting compounds enhance the generation of mouse induced pluripotent stem cells. Aging Cell. 2011; 10: 908-11.
46. Menendez JA, Vellon L, Oliveras-Ferraros C, Cufi S, Vazquez-Martin A. mTOR-regulated senescence and autophagy during reprogramming of somatic cells to pluripotency: a roadmap from energy metabolism to stem cell renewal and aging. Cell Cycle. 2011; 10: 3658-77.
47. Guan JL, Simon AK, Prescott M, Menendez JA, Liu F, Wang F, et al. Autophagy in stem cells. Autophagy. 2013; 9: 830-49.
48. Oliver L, Hue E, Priault M, Vallette FM. Basal autophagy decreased during the differentiation of human adult mesenchymal stem cells. Stem cells and development. 2012; 21: 2779-88.
49. Pantovic A, Krstic A, Janjetovic K, Kocic J, Harhaji-Trajkovic L, Bugarski D, et al. Coordinated time-dependent modulation of AMPK/Akt/mTOR signaling and autophagy controls osteogenic differentiation of human mesenchymal stem cells. Bone. 2013; 52: 524-31.
50. Dang S, Xu H, Xu C, Cai W, Li Q, Cheng Y, et al. Autophagy regulates the therapeutic potential of mesenchymal stem cells in experimental autoimmune encephalomyelitis. Autophagy. 2014; 10: 1301-15.
51. James AW. Review of Signaling Pathways Governing MSC Osteogenic and Adipogenic Differentiation. Scientifica (Cairo). 2013; 2013: 684736.
52. Li S, Kong H, Yao N, Yu Q, Wang P, Lin Y, et al. The role of runt-related transcription factor 2 (Runx2) in the late stage of odontoblast differentiation and dentin formation. Biochemical and biophysical research communications. 2011; 410: 698-704.
53. Pratap J, Galindo M, Zaidi SK, Vradii D, Bhat BM, Robinson JA, et al. Cell growth regulatory role of Runx2 during proliferative expansion of preosteoblasts. Cancer Res. 2003; 63: 5357-62.
54. Marinovich R, Soenjaya Y, Wallace GQ, Zuskov A, Dunkman A, Foster BL, et al. The role of bone sialoprotein in the tendon-bone insertion. Matrix Biol. 2016; 52-54: 325-38.
55. Klionsky DJ, Abdalla FC, Abeliovich H, Abraham RT, Acevedo-Arozena A, Adeli K, et al. Guidelines for the use and interpretation of assays for monitoring autophagy. Autophagy. 2012; 8: 445-544.
56. Pfeilschifter J, Koditz R, Pfohl M, Schatz H. Changes in proinflammatory cytokine activity after menopause. Endocr Rev. 2002; 23: 90-119.
57. Liao L, Su X, Yang X, Hu C, Li B, Lv Y, et al. TNF-alpha Inhibits FoxO1 by Upregulating miR-705 to Aggravate Oxidative Damage in Bone Marrow-Derived Mesenchymal Stem Cells during Osteoporosis. Stem Cells. 2016; 34: 1054-67.
58. Zhao L, Huang J, Zhang H, Wang Y, Matesic LE, Takahata M, et al. Tumor necrosis factor inhibits mesenchymal stem cell differentiation into osteoblasts via the ubiquitin E3 ligase Wwp1. Stem Cells. 2011; 29: 1601-10.
59. Dalle Carbonare L, Valenti MT, Zanatta M, Donatelli L, Lo Cascio V. Circulating mesenchymal stem cells with abnormal osteogenic differentiation in patients with osteoporosis. Arthritis Rheum. 2009; 60: 3356-65.
60. An Y, Liu W, Xue P, Zhang Y, Wang Q, Jin Y. Increased autophagy is required to protect periodontal ligament stem cells from apoptosis in inflammatory microenvironment. J Clin Periodontol. 2016; 43: 618-25.
61. Mitter SK, Song C, Qi X, Mao H, Rao H, Akin D, et al. Dysregulated autophagy in the RPE is associated with increased susceptibility to oxidative stress and AMD. Autophagy. 2014; 10: 1989-2005.
62. Moscat J, Karin M, Diaz-Meco MT. p62 in Cancer: Signaling Adaptor Beyond Autophagy. Cell. 2016; 167: 606-9.
63. Wullschleger S, Loewith R, Hall MN. TOR signaling in growth and metabolism. Cell. 2006; 124: 471-84.
64. Shimobayashi M, Hall MN. Making new contacts: the mTOR network in metabolism and signalling crosstalk. Nat Rev Mol Cell Biol. 2014; 15: 155-62.

65. Duvel K, Yecies JL, Menon S, Raman P, Lipovsky AI, Souza AL, et al. Activation of a metabolic gene regulatory network downstream of mTOR complex 1. Mol Cell. 2010; 39: 171-83.
66. Okayasu I, Hatakeyama S, Yamada M, Ohkusa T, Inagaki Y, Nakaya R. A novel method in the induction of reliable experimental acute and chronic ulcerative colitis in mice. Gastroenterology. 1990; 98: 694-702.
67. Dieleman LA, Palmen MJ, Akol H, Bloemena E, Pena AS, Meuwissen SG, et al. Chronic experimental colitis induced by dextran sulphate sodium (DSS) is characterized by Th1 and Th2 cytokines. Clin Exp Immunol. 1998; 114: 385-91.
68. Wang K, Niu J, Kim H, Kolattukudy PE. Osteoclast precursor differentiation by MCPIP via oxidative stress, endoplasmic reticulum stress, and autophagy. J Mol Cell Biol. 2011; 3: 360-8.
69. DeSelm CJ, Miller BC, Zou W, Beatty WL, van Meel E, Takahata Y, et al. Autophagy proteins regulate the secretory component of osteoclastic bone resorption. Dev Cell. 2011; 21: 966-74.
70. Liu S, Zhu L, Zhang J, Yu J, Cheng X, Peng B. Anti-osteoclastogenic activity of isoliquiritigenin via inhibition of NF-kappaB-dependent autophagic pathway. Biochemical pharmacology. 2016; 106: 82-93.
71. Owen HC, Vanhees I, Gunst J, Van Cromphaut S, Van den Berghe G. Critical illness-induced bone loss is related to deficient autophagy and histone hypomethylation. Intensive Care Med Exp. 2015; 3: 52.
72. Bell A, Grunder L, Sorisky A. Rapamycin inhibits human adipocyte differentiation in primary culture. Obes Res. 2000; 8: 249-54.
73. Chang GR, Chiu YS, Wu YY, Chen WY, Liao JW, Chao TH, et al. Rapamycin protects against high fat diet-induced obesity in C57BL/6J mice. J Pharmacol Sci. 2009; 109: 496-503.